JOURNAL OF MATERIALS SCIENCE **34** (1999) 2987–2996

# A novel preparation method for porous noble metal/ceramic catalytic membranes

HONGBIN ZHAO, ANWU LI, JINGHU GU, GUOXING XIONG*
*State Key Laboratory of Catalysis, Dalian Institute of Chemical Physics, Chinese Academy of Sciences, Dalian 116023, People's Republic of China*

H. BRUNNER
*Fraunhofer Institute for Interfacial Engineering and Biotechnology Nobelstraße 12, D-70569 Stuttgart, Germany*
*E-mail: gxxiong@ms.dicp.ac.cn*

Adsorption at liquid/solid interface has been explored to prepare catalytically active ceramic membranes. Boehmite sol maintains its dynamic stability in the pH range of 3.5–4. Adsorption of metal salt on the sol particles can only be performed in the above pH range, but the adsorption can still be optimized by proper choice of ligand. Therefore, the effect of the ligands ($NH_3$, $Cl^-$, EDTA) on the adsorption of the noble metal ions (Pd(II), Pt(II), Pt(IV) and Rh(III)) as a function of pH on $\gamma$-$Al_2O_3$ particles was studied. Thus the noble metal complexes which can significantly adsorb in the above pH range were found. Using the complexes, the noble metal ion modified boehmite sols were synthesized. Then by the sol-gel process, the porous noble metal/ceramic cataytic membranes were prepared. The membranes were further characterized by $N_2$ adsorption-desorption, scanning electron microscopy (SEM), transmission electron microscopy (TEM) and SEM-WDX (wave dispersion of X-ray). The $H_2$ and $N_2$ permeation through these membranes at elevated temperatures was also measured. Based on the above experiments, the novel technique can produce the mesoporous catalytically active ceramic membranes without any defects and with a uniform dispersion of the active materials in the coating. 

## 1. Introduction

In recent years there has been an increasing interest in using inorganic membranes in the processes of catalytic reactions [1, 2]. These applications are based on the properties of inorganic membranes involving their good structural, chemical and thermal stabilities and potential of being catalytically modified. As far as the role of inorganic membranes in catalytic reactors is concerned, the separation versus non-separation may be recognized [3], depending on whether or not membrane permselectivity is essential in catalytic reactors. The membrane reactor for dehydrogenation is a good example of the separation application, i.e., hydrogen as one of the reaction products is selectively removed by palladium-based membranes, resulting in an increase in the per-pass conversion [4]. For the non-separation application, inorganic membranes act as a chemical contactor to control the way the reactants come into contact, for example separate feed of reactants from opposite membrane sides. This application mainly concerns the enhancement of the reaction selectivity towards target products of some reactions, e.g., hydrogenations [5, 6] and partial oxidations [7]. In the later application, porous inorganic membranes, which most are catalytically modified and usually named catalytically active membranes, were employed. By comparison, the later concept is less investigated and recently has been attracting more interest. This work mainly was motivated by this concept.

As pointed out above, porous catalytic membranes are important to the application of inorganic membranes in catalytic reactions. At present porous inorganic membranes, which are made of ceramic, carbon, glass or stainless steel, are commercially available. The pore sizes in diameter range from micrometer down to nanometer. They are mainly applied for liquid filtration. Regarding catalytic applications, porous ceramic membranes are more suitable as support for catalysts. Catalytically active materials can be introduced to the membranes by impregnation, precipitation-deposition, ion-exchange, grafting, metallic cluster deposition and sol-gel methods of which recent studies are summarized in Table I. The catalytic modification of porous inorganic membranes may be divided into modification of inert membranes (post-modification) and into incorporation of catalytic materials during preparation

* Author to whom all correspondence should be addressed.

TABLE I Synthesis of porous metal catalytic membranes and their applications

| Catalytic membrane | Synthesis method | Application | Reference |
|---|---|---|---|
| Pd/anodic | Impregnation | $H_2$ separation | [16] |
| Pt/Vycor glass | Impregnation | Dehydrogenation | [9] |
| Pd/Vycor glass | Impregnation | $H_2$ separation | [17] |
| Pt/$\gamma$-$Al_2O_3$ | Incipient impregnation | Dehydrogenation | [10] |
| Pt/$\gamma$-$Al_2O_3$ | Impregnation | | [18] |
| Pd/$\gamma$-$Al_2O_3$ | Impregnation | $H_2$ separation | [19] |
| Ni/$\gamma$-$Al_2O_3$ | Impregnation | Hydrogenation | [20] |
| Ag/$\gamma$-$Al_2O_3$ | Reservoir method | $O_2$ permeation | [21] |
| Pt/$\gamma$-$Al_2O_3$ | Reservoir method | | [11] |
| Pt/$\gamma$-$Al_2O_3$ | Ion-exchange | Hydrogenation | [12] |
| Rh/$SiO_2$ | Grafting | | [22] |
| Pt/$\gamma$-$Al_2O_3$ | Cluster deposition | Hydrogenation | [23] |
| Pt/$\gamma$-$Al_2O_3$ | Sol-gel method | | [13] |
| Metals/$\gamma$-$Al_2O_3$ | Sol-gel method | $H_2$ separation | [14] |
| Ru/$SiO_2$ | Sol-gel method | Partical oxidation | [15] |
| Ni/$\gamma$-$Al_2O_3$ | Sol-gel method | Methanol Decomposition | [24] |
| Pd/$\gamma$-$Al_2O_3$ | Sol-gel method | $H_2$ separation | [25] |

of inorganic membranes (*in-situ* modification). Sol-gel method belongs to the *in-situ* modification method, while the other methods listed in Table I are post modification method. Recently, Yang and Xiong gave a comprehensive review of catalytic modification of porous inorganic membranes [8].

In the work of Sun and Khang [9], an impregnation procedure was performed by dipping porous Vycor membranes into a chloroplatinic acid solution followed by heat treatment and activation. It appeared that the catalyst was distributed in the whole membrane. Champagnie *et al.* [10] prepared Pt/$\gamma$-$Al_2O_3$ catalytic membranes by incipient wetness impregnation, i.e., with a micropipette impregnation solution was dropped into the inside surface of the membrane. Energy dispersive X-ray spectroscopy analysis indicated that Pt was deposited both in the $\gamma$-$Al_2O_3$ layer and in the two intermediate alumina layers. According to the work of Luyten *et al.* [11], the reservoir method, i.e., a precipitation-deposition method, could be used to realize Pt/$\gamma$-$Al_2O_3$ catalytic membranes where most of the catalyst is loaded in the top layer. An ion exchange method was used to incorporate Pt into porous alumina membranes. It was confirmed that Pt was mainly deposited in the $\gamma$-$Al_2O_3$ layer [12]. Based on the above overview of the post-modification methods, these techniques can not always be used to yield the desired active phase loading and location in membrane supports. In addition, these techniques do not guarantee uniform catalyst loading along the length of the membrane supports [13]. Therefore, it is worthwhile to consider alternative methods.

Yeung *et al.* [13] developed a new strategy for making porous catalytic membranes using a sequential slip-casting technique, i.e., a multiple sol-gel process. Followed the procedure reported, a boehmite sol or a chloroplatinic acid impregnated sol was deposited on a porous $\alpha$-$Al_2O_3$ substrate by slip-casting followed by heat treatment and activation. The desired distribution of Pt/$\gamma$-$Al_2O_3$ layers within the membrane was obtained by varying the thickness of the slip-casting layers as well as their arrangement, resulting in uniform or nonuniform catalyst distribution within the membranes. It was claimed that the precise control over the active layer thickness and location can be realized. However, their report did not give the experimental determination of the catalyst location. Using the sol-gel method, Chai *et al.* [14] prepared metal-dispersed alumina membranes for a membrane reactor for $CH_4$ steam reforming, the metals included Pt, Pd, Ru and Rh. Transmission electron microscopy shows that the typical particle size of rhodium deposited in the alumina membrane was about 5 nm in diameter. This shows that sol-gel method can be used to obtain catalytic membranes with a high dispersion of catalytically active phases. Pârvulescu *et al.* [15] reported the preparation of ruthenium silica membranes by the sol-gel process. In their work, it was proposed that the use of surfactant (e.g., tetra-alkylammonium salts) in the sol can enhance the dispersion of the catalytic species. In addition, it was suggested that the ruthenium-silica interactions through the formation of Si-O-Ru bonds acts positively on the dispersion of the catalytic species. However, it should be mentioned that the presence of the surfactant induced a decrease in specific surface area and an increase in pore size of the membrane materials.

On the basis of the overview of the preparation of porous metal-based catalytic membranes mainly by impregnation and sol-gel method, the sol-gel method can become an alternative to the impregnation method. However, the characterization of sol-gel derived catalytic membranes has not been performed exclusively.

In this work, the sol-gel method was further explored to prepare porous catalytic $\gamma$-$Al_2O_3$ membranes. The distribution of catalytic materials in the membranes was determined and the $H_2$ transport property of this type of the membranes was studied.

In the sol-gel process applied, the adsorption of catalytically active precursor, usually metal salt, at liquid/solid interface was addressed. The objective is locate the catalytically active phases and to improve their dispersion. For the preparation of $\gamma$-$Al_2O_3$ membranes,

the sol-gel procedure mainly consists of synthesis of the boehmite sol, sol-casting on a porous substrate followed by drying and calcination steps. The catalytically active precursor may be introduced to the boehmite sol. The adsorption of the metal salt may take place by the surface OH groups of the boehmite sol particles. In principle, the adsorption can be optimized by the pH of the metal salt-boehmite sol. However, it should be mentioned that the boehmite sol maintains its dynamic stability in the pH range of 3.5–4. Accordingly, the adsorption can only be performed in the above pH range. Therefore, we proposed that the adsorption can still be optimized by proper choice of ligand. The search of the ligand was performed by the measurement of the adsorption as a function of pH. Then, according to the adsorption versus pH curves, the ligand, which can enhance the adsorption of metal salt in the pH range of 3.5–4, was determined. It should be noted that the above measurements were made in a system of the metal salt-ligand-$\gamma$-$Al_2O_3$ powder not in a system of the metal salt-ligand-boehmite sol since beyond the above pH range the boehmite sol loses its stability. Qualitatively, the result can be applied to a system of the metal salt-ligand-boehmite sol because the surface OH groups of the $\gamma$-$Al_2O_3$ particles could be comparable to those of the boehmite sol particles.

## 2. Experimental

### 2.1. Determination of the amount of adsorption as a function of pH

$\gamma$-$Al_2O_3$ powder was obtained by calcining at 600 °C commercial PURAL SB powder (Condea Chemice GmbH), which mainly contained a phase of boehmite. The calcined powder has a specific surface area of 233 $m^2$/g, a pore volume of 0.47 ml/g and an average pore diameter of 5.7 nm.

In the adsorption experiments, the system metal salt-ligand-$\gamma$-$Al_2O_3$ powder consisted of 100 ml of a $10^{-4}$ mol/l solution of the metal salt with the ligand studied and 0.3 g of the $\gamma$-$Al_2O_3$ powder together in a conical flask. The surface hydroxyl group density of $\gamma$-$Al_2O_3$ particles in aqueous solutions is often taken to be 8 OH/$nm^2$ [26] and this value is used here. The amount of the metal salt corresponds to about 0.2% of the surface OH groups of the alumina in the suspension. The suspension was adjusted to the desired pH value using $HNO_3$ and NaOH. In this way, all fifteen samples were prepared. The pH values of the samples were distributed in the pH range of 1–10 and the pH difference between two neighboring samples remained about 0.5 pH unit. The samples were shaken at room temperature in order to attain chemical equilibrium of the adsorption. After 4–6 h shaking, the pH values of the samples were measured. The solutions were separated by centrifugation and the concentration of the metal salt was measured by a spectrophotometric method.

The adsorption data were presented by the following equation:

$$E\% = \frac{M_{\text{total}} - M_{\text{left}}}{M_{\text{total}}} \times 100$$

where $E\%$ is the amount of adsorption in percentage, $M_{\text{total}}$ is the total amount of the metal salt added, and $M_{\text{left}}$ is the amount of the metal salt left in solution after adsorption equilibrium. As seen in the above equation, the adsorption percentage is a function of the original solution concentration. In this work, the adsorption experiments were performed in the area of low surface loading of the metal salt on the alumina powder and with a constant concentration of the metal salt. In this way, the adsorption substantially changed as a function of the parameters studied (ligand and pH). Thus the effect of the ligands on the adsorption of the metal salts can be determined in the desired pH range.

### 2.2. Preparation of porous noble metal/ceramic catalytic membranes

The preparation of porous noble metal/ceramic catalytic membranes is schematically shown in Fig. 1. A boehmite sol was produced by peptization of the suspension of the boehmite powder. The peptization was performed with a molar $H^+/Al^{3+}$ ratio of 0.09 at 80 °C for 5 h. Then the desired metal complex was introduced into the sol. The viscosity of the catalytically modified sol was adapted with polyvinylacohol 72000 (PVA) and polyethyleneglycol 400 (PEG). PVA and PEG can also enhance the strength of gel-coating to prevent crack formation during drying and calcination. In this work, a typical casting sol consisted of the catalytically modified sol with 0.5 mol/l aluminium and with 2–5 wt % PVA and PEG. Commercial porous $\alpha$-$Al_2O_3$ discs with an average pore diameter of 1.6 $\mu$m and 48% porosity were used as substrates. The sol was deposited on the substrate by a dip coating technique, i.e., one side of the substrate was contacted with the sol for 8–10 s. Immediately after the dipping, the coated substrate was spun at 500–600 rpm. This spinning removed excess sol which would otherwise give a less uniform coating. The coating was dried at 5 °C and 65% relative humidity for two days, followed by calcination at 600 °C for 3 h with a heating and cooling rate smaller than 1 °C/min. As seen above, the coating process of the sol-gel method

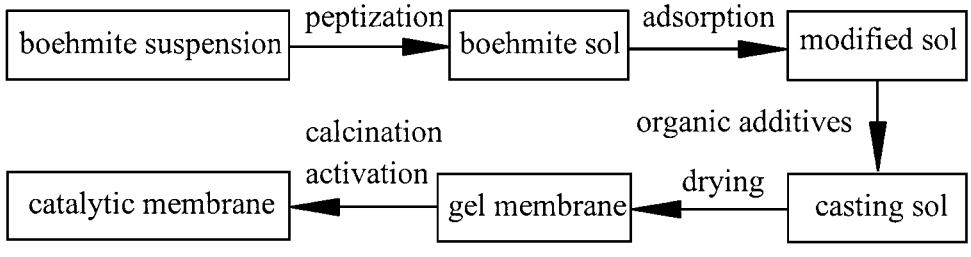


*Figure 1* Schematic of the preparation of porous noble metal/ceramic catalytic membrane.

mainly consisted of dip coating, drying and calcination steps. These steps were repeated to increase membrane thickness; this procedure was named multiple sol-gel process in this work.

Using the sol-gel method with the same conditions applied for the membranes but without the dip coating step, membrane materials were prepared for characterization.

The loading amount of the catalytically active component was obtained by calculation based on the catalytic component and aluminium content of the membrane material and is given in metal/$\gamma$-$Al_2O_3$ by weight.

### 2.3. Catalytic membrane characterization

The particle size of the sols was measured by photocorrelation spectroscopy (Malvern Zetasizer 3). The as-prepared sols need to be diluted with distilled water to obtain a dilute dispersion system.

The $N_2$ adsorption-desorption isotherms of the membrane materials at 77 K were obtained by a static volumetric method with the ASAP 2000 (Micrometerics). The specific surface area of the membrane materials was calculated on the basis of the Brunauer, Emmett and Teller theory (BET) using the adsorption isotherm. The pore diameter and pore diameter distribution were calculated based on the Barrett, Joyner and Halenda theory (BJH) from the desorption isotherm [27].

The morphologies of the membranes were examined by scanning electron microscopy (SEM Stereoscan 120).

The metal distribution in the membranes was determined by scanning electron microscopy-wave dispersive X-ray analyzer (SEM-WDX) (WDX Mapping S200).

The metal particle size of the membrane materials was observed by transmission electron microscopy (TEM Jeol-100C). The membrane material was grounded and dispersed in an ethanol solvent by ultrasound. One drop of the suspension was transferred onto a copper grid coated with carbon.

The pure gas ($H_2$ or $N_2$) permeation through the membranes was determined using a stationary method. In this method, the pressure at the permeation side is fixed, normally at atmospheric pressure and the pressure at the feeding side is set higher than atmospheric pressure. At steady state, the gas flux is measured with a bubble flow meter. The coated disc has a diameter of 30 mm and a thickness of 1 mm. The side edge of the disc was sealed by commercial ceramic glass (UHLIG Kera-Dekor), which can resist to high temperature up to 800 °C. A laboratory made stainless steel permeation cell was employed. The disc was fixed in the cell with graphite gaskets. Before the permeation measurement, the coated disc was treated with $H_2$ at 500 °C overnight.

## 3. Results and discussion

### 3.1. Metal complexes for modification of boehmite sol and modified sols

Boehmite sol maintains its dynamic stability in the pH range of 3.5–4. Adsorption of the metal ions on the boehmite sol particles can only be performed in the above pH range, but the adsorption can still be optimized by proper choice of ligand. Therefore, the effect of the ligands ($Cl^-$, $NH_3$ and EDTA) on the adsorption at the liquid/solid interface was studied. It is well known that alumina supported noble metals (Pd, Pt and Rh) have become one of the most important industrial catalysts. Thus, the adsorption of Pd(II), Pt(II), Pt(IV) and Rh(III) was involved in this study.

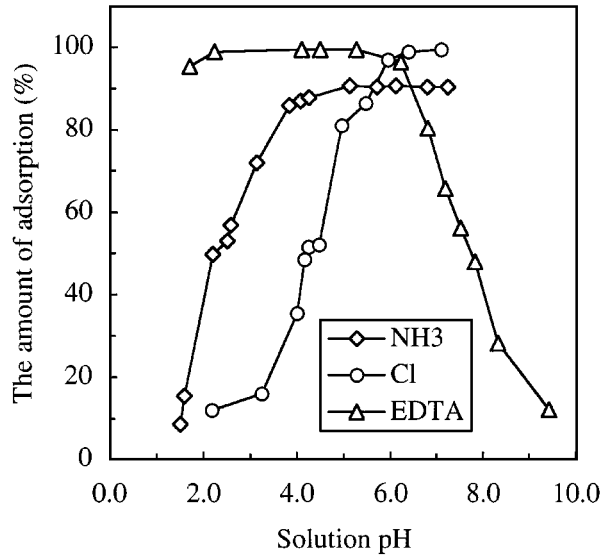


*Figure 2* Adsorption percentage of Pd(II) complexes as a function of pH (the initial solution concentration of Pd(II): $2–3 \times 10^{-4}$ mol/l, Pd(II) complexes used: $PdCl_4^{2-}$, $Pd(NH_3)_4^{2+}$ and $PdEDTA^{2-}$).

The surface of $\gamma$-$Al_2O_3$ particles in an aqueous solution is hydrated and the surface OH groups of the $\gamma$-$Al_2O_3$ particles can be formed [28]. Qualitatively, the surface OH groups of the hydrated $\gamma$-$Al_2O_3$ particles are comparable to those of the boehmite sol particles. Therefore, the respective interactions at the liquid/solid interface could be comparable to each other. Accordingly, the conclusions of the above study could also be applied to a system metal ions-ligand-boehmite sol.

Fig. 2 shows the adsorption of three kinds of the Pd(II) complexes as a function of pH. From Fig. 2, the adsorption percentages of $Pd(NH_3)_4^{2+}$ and $PdEDTA^{2-}$ reach more than 80% in the pH range of 3.5–4. Fig. 3a and b give the adsorption percentages of one Pt(IV) and three Pt(II) complexes as a function of pH, respectively. As indicated in Fig. 3, the adsorption of $PtCl_6^{2-}$, $PtCl_4^{2-}$ and $PtEDTA^{2-}$ took place in the above pH range significantly. Fig. 4 shows the adsorption percentages of $RhCl_6^{3-}$ as a function of pH. As seen in Fig. 4, the adsorption percentages of $RhCl_6^{3-}$ become as much as 85% in the pH range of 3.5–4. In summary, $Pd(NH_3)_4^{2+}$, $PdEDTA^{2-}$, $PtCl_6^{2-}$, $PtCl_4^{2-}$, $PtEDTA^{2-}$, and $RhCl_6^{3-}$ can adsorb significantly on the $\gamma$-$Al_2O_3$ particles in the pH range where the boehmite sol will be stable. This means that these complexes could be used for the modification of the boehmite sol by adsorption at the liquid/solid interface.

The ligands of $Cl^-$, $NH_3$ and EDTA were shown to have a remarkable effect on the adsorption of the metal ions (Pd(II), Pt(II), Pt(VI) and Rh(III)). As a consequence, ligands can be used to tailor adsorption at the liquid/solid interface to a specific application like pH.

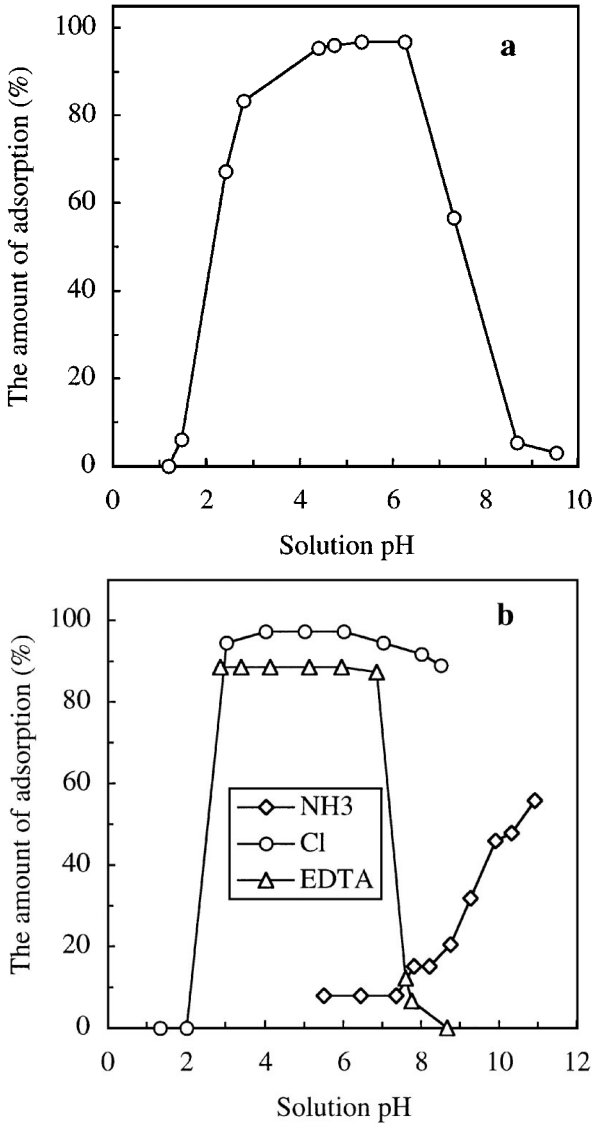


*Figure 3* Adsorption percentage of Pt(IV) and Pt(II) complexes as a function of pH: (a) Pt(IV) (the initial solution concentration of Pt (IV): $4–5 \times 10^{-5}$ mol/l, Pt(IV) complex used: $PtCl_6^{2-}$), (b) Pt(II) (the initial solution concentration of Pt(II): $4–5 \times 10^{-5}$ mol/l, Pt(II) complexes used: $PtCl_4^{2-}$, $Pt(NH_3)_4^{2+}$ and $PtEDTA^{2-}$).

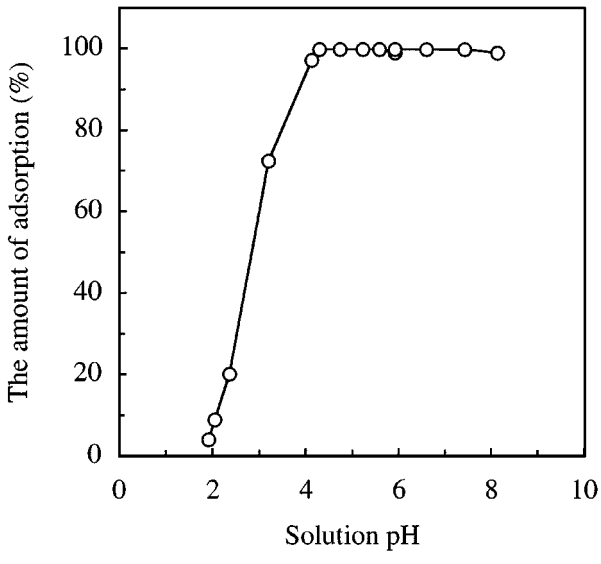


*Figure 4* Adsorption percentage of Rh(III) complex as a function of pH (the initial solution concentration of Rh(III): $4–5 \times 10^{-4}$ mol/l, Rh(III) complexe used: $RhCl_6^{3-}$).

It should be noted that the adsorption versus pH curves in Figs 2–4 fall into three categories, i.e., the adsorption percentage increases and then remains more or less unchanged with pH, named S-curve; the adsorption percentage remains constant and then sharply decreases with pH, named reverse S-curve; the adsorption percentage exhibits a maximum with pH, called composite curve (C-curve). Qualitative studies of noble metal adsorption onto alumina and/or silica suggest that the adsorption can be attributed to an electrostatic force. At pH values below the oxide's point of zero charge (PZC), the terminal hydroxyl groups at the oxide surface become protonated and so positively charged and capable of adsorbing anions, and vice versa as pH is raised above the ZPC. On the basis of the above electrostatic model, these curves can not be explained. We suggest that chemical interactions, e.g., surface complexing, are mainly responsible for the adsorption at the liquid/solid interface in this study. In our further work, this will be investigated in detail.

The effects of the introduction of $Pd(NH_3)_4^{2+}$ solution to the boehmite sol were examined. With the introduction of the dopant, it was not found that the aggregation of the doped sol took place in one week. Fig. 5 shows the particle diameter distribution of the modified sol with 2 wt % Pd. As seen in Fig. 5, the modified sol still exhibits a narrow particle diameter distribution. This means that a modified boehmite sol with dynamic stability and a narrow particle diameter distribution can be obtained by the procedure proposed.

Table II lists the average particle diameter of the modified sols as a function of the content of $Pd(NH_3)_4^{2+}$. The average particle diameter of the modified sols increased

TABLE II The particle size of Pd(II)-modified boehmite sol[a]

| Pd content (wt % in Pd/$\gamma$-$Al_2O_3$) | Sol particle diameter (nm) |
|---|---|
| 1 | 43.7 |
| 2 | 66.2 |
| 3 | 73.0 |
| 4 | 59.5 |

[a] $Pd(NH_3)_4^{2+}$ was used as palladium precursor.

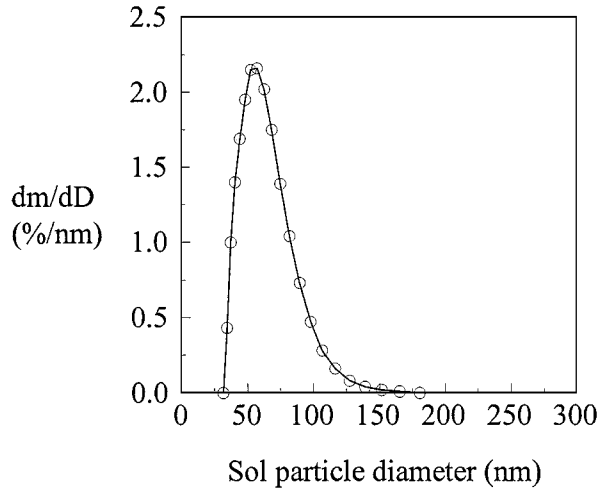


*Figure 5* Particle diameter distribution of the Pd(II)-modified boehmite sol ($Pd(NH_3)_4^{2+}$ was used as palladium precursor, the content of palladium in the sol: 4 wt % in Pd/$\gamma$-$Al_2O_3$).

with the content of $Pd(NH_3)_4^{2+}$. This could be attributed to the adsorption of $Pd(NH_3)_4^{2+}$ on the boehmite sol particles. It should be mentioned that the modified boehmite sol with 4 wt % Pd exhibited a smaller particle diameter than that of the 3 wt % sol. This remains questionable.

### 3.2. Structure of catalytic membranes

In this work, $Pd(NH_3)_4^{2+}$, $PtCl_6^{2-}$ and $RhCl_6^{3-}$ were used to obtain their respective modified boehmite sols. The multiple sol-gel process was applied to prepare thick catalytic membranes and for each type of catalytic membrane the same casting sol was used to do all the dip coatings. Fig. 6 shows the SEM micrographs of the cross section of the Pd/$\gamma$-$Al_2O_3$, Pt/$\gamma$-$Al_2O_3$ and Rh/$\gamma$-$Al_2O_3$ membrane prepared by performing the sol-gel process six times. The thickness of the Pd/$\gamma$-$Al_2O_3$, Pt/$\gamma$-$Al_2O_3$ and Rh/$\gamma$-$Al_2O_3$ membrane grew to about 16, 14 and 12 $\mu$m by the six-time sol-gel process, respectively. The interfaces among the six successive layers were not recognized. However, Zaspalis [29] found the interfaces among the successive $TiO_2$ layers produced by a multiple sol-gel process. In addition, any cracks and pinholes of the above catalytic membranes investigated by SEM were not observed.

Fig. 7 shows the thickness of the Pd/$\gamma$-$Al_2O_3$ membrane as a function of the number of successive dipping. As seen in Fig. 7, the thickness increases linearly for the initial four dippings and then the increase in thickness becomes less and less for the last two dippings. The multiple sol-gel process was also applied both in the

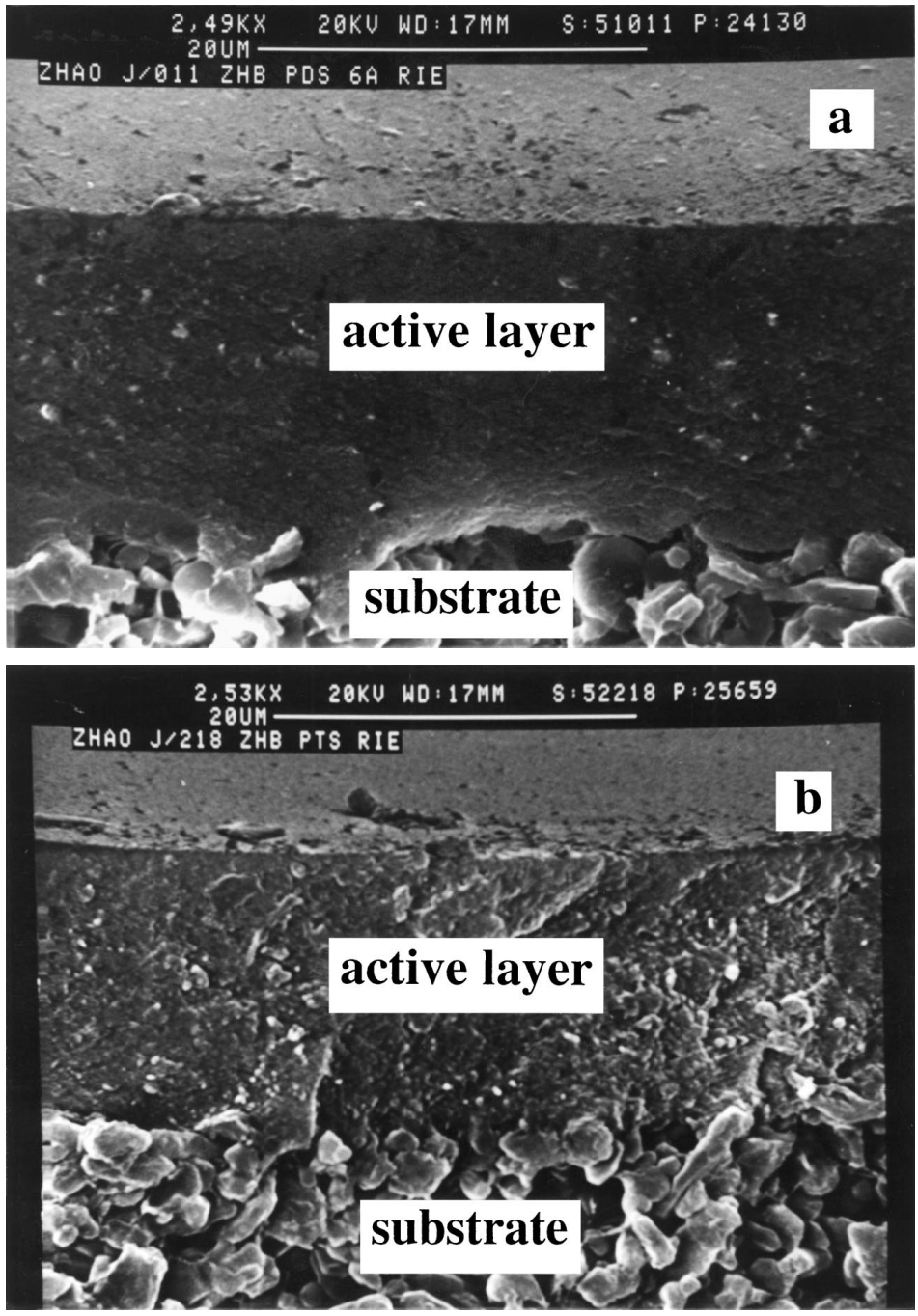


*Figure 6* SEM micrographs of the cross-section of the membranes prepared by six-time dipping: (a) Pd/$\gamma$-$Al_2O_3$, (b) Pt/$\gamma$-$Al_2O_3$, and (c) Rh/$\gamma$-$Al_2O_3$ (all the membrane materials contained 4 wt % in metal/$\gamma$-$Al_2O_3$, respectively). (*Continued.)*

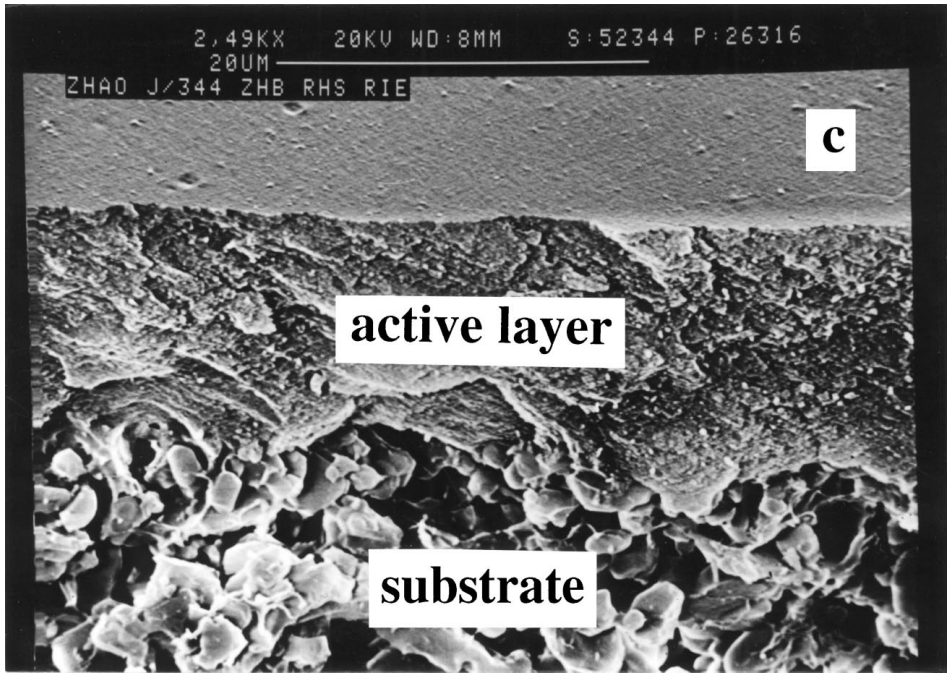


*Figure 6* (*Continued.*)

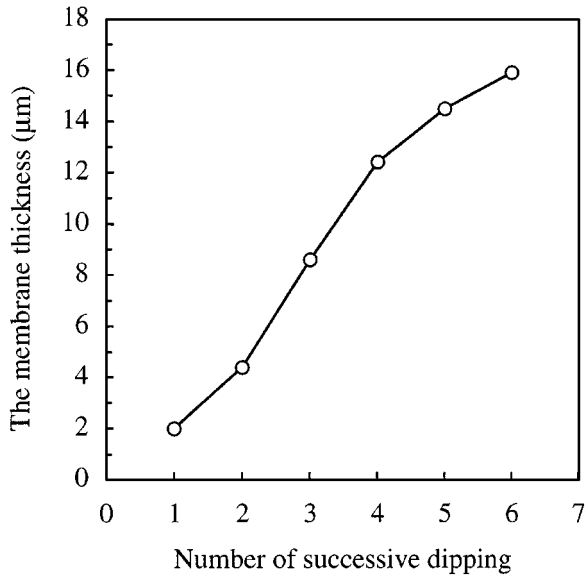


*Figure 7* The thickness of the Pd/$\gamma$-$Al_2O_3$ membrane as a function of dipping times (the content of palladium in the membrane material: 4 wt % in Pd/$\gamma$-$Al_2O_3$).

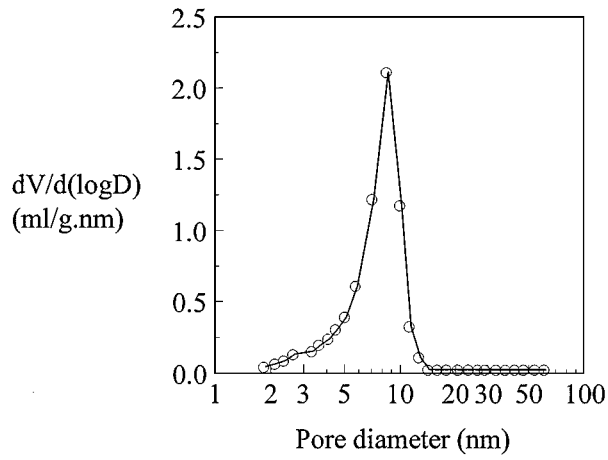


*Figure 8* Pore diameter distribution of the Pd/$\gamma$-$Al_2O_3$ membrane material (the content of palladium in the membrane material: 2 wt % in Pd/$\gamma$-$Al_2O_3$).

work of Yeung *et al.* [13] and the work of Chai *et al.* [14]. Yeung reported the preparation of Pt/$\gamma$-$Al_2O_3$ membranes with a thickness of 1–11 $\mu$m, but did not give details of the preparation. In the work of Chai *et al.* the process was repeated 25–40 times, resulting in membranes with a thickness of about 10–20 $\mu$m. According to our work, the thickness of the catalytic membranes prepared by each individual sol-gel process is mainly a function of the concentration of the boehmite sol, the metal salt, the viscosity of the casting sol (which can be modified by PVA and PEG) and the porous substrate. It is evident that the multiple sol-gel process can be used to obtain a thick catalytic membrane without any defects and further to tailor the thickness of the catalytic membrane.

The pore structure of Pd/$\gamma$-$Al_2O_3$ membrane materials with various loading of Pd was determined. Fig. 8 shows the pore diameter distribution of the Pd/$\gamma$-$Al_2O_3$ membrane materials (2 wt % Pd). As expected by the particle packing model [30], a porous Pd/$\gamma$-$Al_2O_3$ membrane material with a narrow pore diameter distribution was made from its precursor the Pd(II)-modified boehmite sol with a narrow particle diameter distribution as shown in Fig. 5.

Table III lists the average pore diameters and BET specific surface areas of the Pd/$\gamma$-$Al_2O_3$ membrane

TABLE III The pore structure of Pd/$\gamma$-$Al_2O_3$ membrane material

| Pd content (wt % in Pd/$\gamma$-$Al_2O_3$) | Pore diameter (nm) | BET surface area ($m^2$/g) |
|---|---|---|
| 0.5 | 5.48 | 267 |
| 1.0 | 5.56 | 271 |
| 1.5 | 6.45 | 240 |
| 2.0 | 6.47 | 253 |

materials. The pore diameter of the Pd/$\gamma$-$Al_2O_3$ membrane material increases slightly with the Pd content. The BET specific surface area exhibits a decrease with the Pd content. It is evident that the introduction of Pd in the sol-gel process has an effect on the pore structure of the membrane material. This observation is in agreement with our above proposal that the adsorption of Pd(II) on the boehmite sol particles resulted in an increase in the particle diameter of the modified sols.

Fig. 9 shows the SEM-WDX result for the Pd/$\gamma$-$Al_2O_3$ membrane with 4 wt % Pd prepared by the six-time sol-gel process. The right side is the SEM micrograph of the membrane and the left side shows the WDX result of the corresponding membrane. The white dots represent the WDX mapping for the element Pd. The distribution of the white dots displays a sharp interface between the coating and the substrate with Pd located in the coating. This result indicates that the penetration of the Pd(II) from the Pd(II)-modified sol to the substrate during dip coating was prevented. This can be attributed to the adsorption of $Pd(NH_3)_4^{2+}$ on the boehmite sol particles. In addition, Pd exhibits uniform loading along the length of the membrane as well as in the direction of the membrane thickness.

Fig. 10 shows the TEM micrograph of the Pd/$\gamma$-$Al_2O_3$ membrane material with 4 wt % Pd. As seen

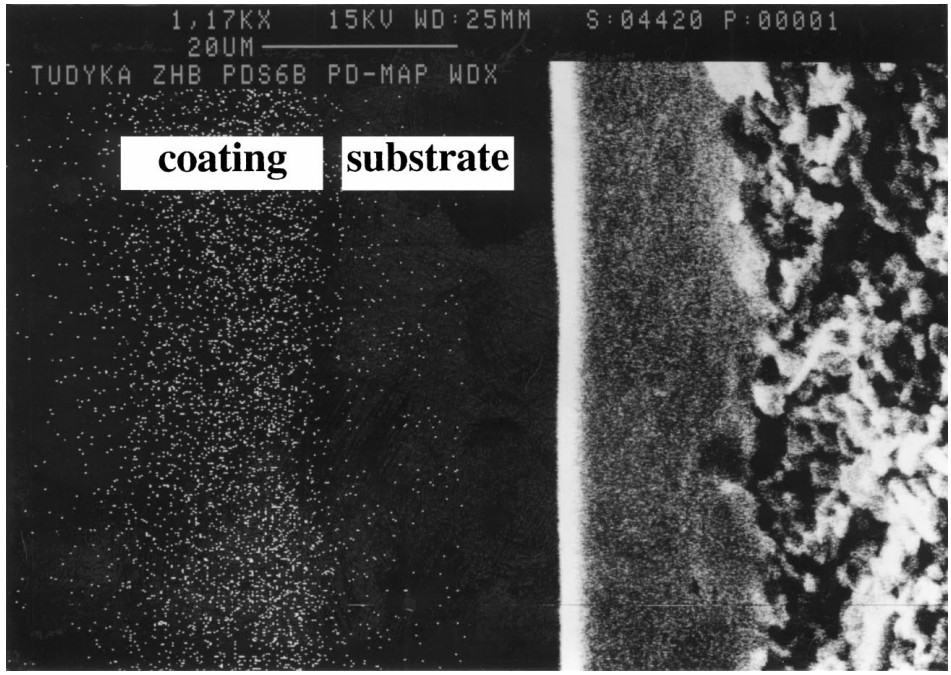


*Figure 9* SEM-WDX micrograph of the cross-section of the Pd/$\gamma$-$Al_2O_3$ membrane prepared by six-time dipping (the content of palladium in the membrane material: 4 wt % in Pd/$\gamma$-$Al_2O_3$).

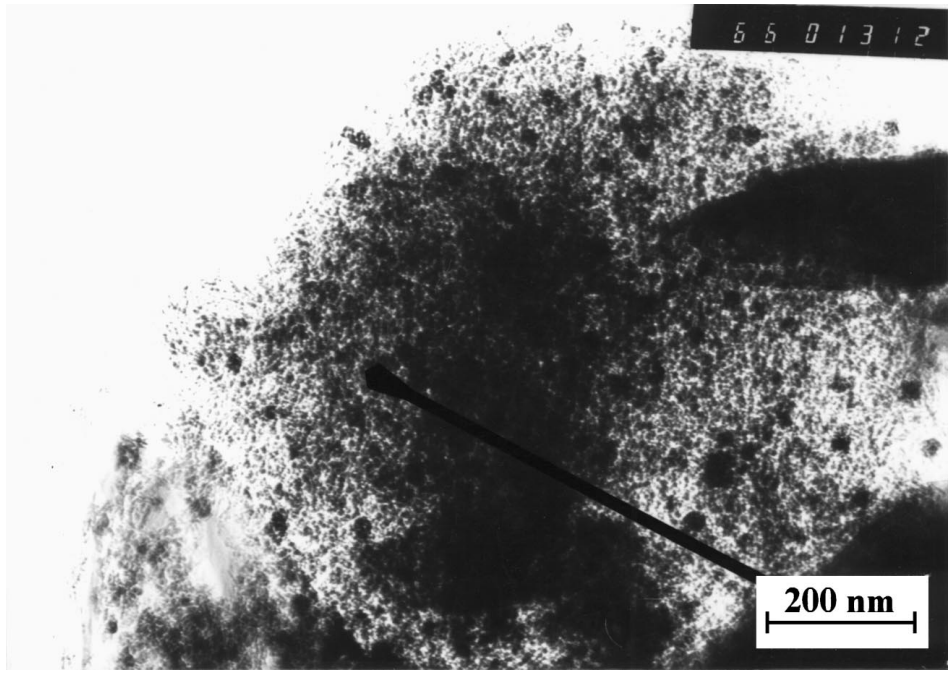


*Figure 10* TEM micrograph of the Pd/$\gamma$-$Al_2O_3$ membrane material (the content of palladium in the membrane material: 4 wt % in Pd/$\gamma$-$Al_2O_3$).

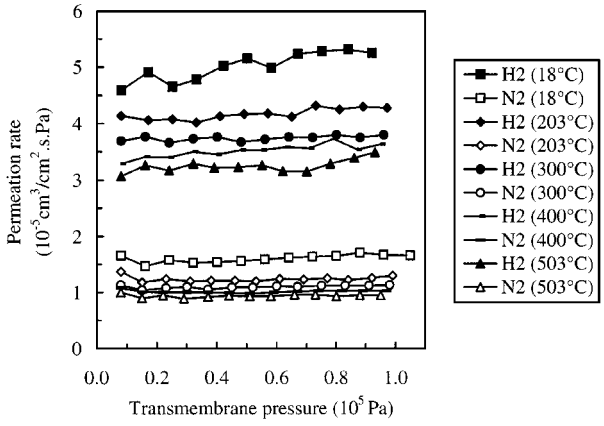


*Figure 11* Gas permeation rate through the Pd/$\gamma$-$Al_2O_3$ membrane prepared by six-time dipping as a function of pressure at various temperatures (the content of palladium in the membrane: 4 wt % in Pd/$\gamma$-$Al_2O_3$).

in Fig. 10, the palladium particles are on average about 10 nm in diameter.

### 3.3. The hydrogen transport properties of the catalytic membrane

Pd/$\gamma$-$Al_2O_3$ membranes were prepared by six-time dipping for the permeation experiment. The effect of the transmembrane pressure and temperature on the $H_2$ and $N_2$ permeation was investigated. Fig. 11 shows the result. As seen in Fig. 11, the permeation rates of $H_2$ decrease with increasing temperature. The rates exhibit slight increase as a function of transmembrane pressure and this could be attributed to the any slight leakage of the system applied. According to the gas transport theory in a porous medium [21], the Knudsen diffusion takes place when the mean free path of a gas molecule is larger than the pore diameter of the porous medium. As shown in Table III, the average pore diameter of the Pd/$\gamma$-$Al_2O_3$ membrane material is about 6 nm. The mean free path of $H_2$ at the investigated condition is 60 nm. It is evident that the Knudsen diffusion can dominate the $H_2$ permeation in the membrane investigated. The Knudsen diffusion coefficient is given as follows

$$F_{k0} = \frac{4\sqrt{2}\varepsilon r}{3\tau_k\sqrt{\pi MRTL}}$$

where $\varepsilon$ is the porosity of the porous medium, $\tau_k$ the tortuosity for Knudsen flow, $r$ is the average pore diameter of the porous medium, $L$ is the thickness of the porous medium, $M$ is the gas molecular weight, $T$ is the temperature and $R$ is the gas constant. From this equation, the Knudsen diffusion decreases with increasing temperature, and is independent of pressure. Accordingly, the effects of temperature and transmembrane pressure observed in this study can be understood.

The observed ratios of $H_2$ to $N_2$ permeation rate are 3.13–3.46 at the five temperatures investigated. The Knudsen permeability ratio of $H_2$ to $N_2$ is 3.74. According to the gas transport theory in a porous medium [21], the presence of surface diffusion can be detected as an extra contribution to gas separation over the Knudsen diffusion. However, this did not occur with this membrane. Therefore, it is suggested that the surface diffusion of $H_2$ in the Pd/$\gamma$-$Al_2O_3$ membrane did not make significant contribution to $H_2/N_2$ separation. This is in agreement with the above observation.

## 4. Conclusion

A novel sol-gel process has been developed, in which the sol can be surface-modified by using a proper metal complex as catalytically active precursor. The novel sol-gel process can be applied to prepare porous noble metal/ceramic catalytic membranes. The resulting Pd/$\gamma$-$Al_2O_3$ membrane exhibits a narrow pore diameter distribution with an average pore diameter of 6 nm up to a metal loading of 4 wt %. Pd is uniformly distributed in the coating of the Pd/$\gamma$-$Al_2O_3$ membrane. The dipping-drying-calcination steps of the sol-gel process can be repeated to obtain a thick catalytic membrane without any defects.

## Acknowledgement

Support for this research work by the National Sciences Foundation of China, German BMBF, FhG-IGB is gratefully acknowledged. The authors wish to thank Miss M. Riedle for taking SEM micrographs, Mr. S. Tudyka for helping with SEM-WDX analysis and Mr. S.-S. Sheng for constructing the gas permeation set-up.

## References

1. J. N. ARMOR, *Appl. Catal.* **49** (1989) 1.
2. G. SARACCO and V. SPECHIA, *Catal. Rev.-Sci. Eng.* **36** (1994) 305.
3. *Idem.*, in "Structured Catalysts and Reactor" (Marcel Dekker, New York, 1998) p. 463.
4. N. ITOH, *AIChE J.* **33** (1987) 1576.
5. P.CINI and M.P.HAROLD, *ibid.* **37** (1991) 997.
6. C.LANGE, S.STORCK, B.TESCHE and W.F.MAIER, *J. Catal.* **175** (1998) 280.
7. V. PÂRVULESCU, V. I. PÂRVULESCU, C. NICULAE and G. POPESCU, *Catal. Today*, in press.
8. W.-S. YANG and G.-X. XIONG, *Current Opinion in Solid State & Materials Science*, in press.
9. Y.-M. SUN and S.-J. KHANG, *Ind. Eng. Chem. Res.* **27** (1998) 1136.
10. A. M. CHAMPAGNIE, T. T. TSOTSIS, R. G. MINET and E. WAGNER, *J. Catal.* **134** (1992) 713.
11. J. LUYTEN, S. VERCAUTEREN, H. WEYTEN, K. VERCAMMEN and R. LEYSEN, in Proceedings of the Third International Conference on Inorganic Membranes, edited by Y.-H. Ma (Worcester, USA, July 1994) p. 405.
12. D. UZIO, J. PEUREUX, A. GIROIR-FENDLER, M. TORRES, J. RAMSAY and J.-A. DALMON, *Appl. Catal. A: General* **96** (1993) 83.
13. K. L. YEUNG, R. ARAVIND, R. J. X. ZAWADA, J. SZEGNER, G. CAO and A. VARMA, *Chem. Eng. Sci.* **49** (1994) 4823.
14. M. CHAI, M. MACHIDA, K. EGUCHI and H. ARAI, *Appl. Catal. A: General* **110** (1994) 239.
15. V. PÂRVULESCU, V. I. PÂRVULESCU, C. NICULAE and G. POPESCU, A. JULBE, C. GUIZARD and L. COT, *Studies in Surface Science and Catalysis* **118** (1998) 205.
16. M.KONNO, M.SHINDO, S.SUGAWARA and S.SAITO, *J. Membr. Sci.* **37** (1988) 193.

17. K. C. CANNON and J. J. HACSKAYLO, *ibid.* **65** (1992) 259.
18. J. W. VELDSINK, G. F. VERSTEEG and W. P. M. VAN SWAAIJ, *ibid.* **92** (1994) 275.
19. S.-Y. LEE, S.-J. LEE, S.-J. KWON, S.-M. YANG and S.-B. PARK, *ibid.* **108** (1995) 97.
20. X. XU, H. VONK, A. C. J. M. VAN DE RIET, A. CYBULSKI and A. STANKIEWICZ, *Catal. Today* **30** (1996) 91.
21. R. J. R. UHLHORN, K. KEIZER and A. J. BURGGRAAF, *J. Membr. Sci.* **46** (1989) 225.
22. N. K. RAMAN, T. L. WARD, C. J. BRINKER, R. SEHGAL, D. M. SMITH, Z. DUAN, M. HANPDEN-SMITH, J. K. BAILEY and J. J. HEADLEY, *Appl. Catal. A: General* **96** (1993) 63.
23. A. N. KARAVANOV, V. M. GRYAZNOV, V. I. LEBEDEVA, I. A. LITVINOV, A. YU. VASIL'LOV and A. YU. OLENIN, *Catal. Today* **25** (1995) 447.
24. T. OKUBO, M. WATANABE, K. KUSAKABE and S. MOROOKA, *Key Eng. Mater.* **61/62** (1991) 71.
25. S.-J. LEE, S.-M. YANG and S.-B. PARK, *J. Membr. Sci.* **96** (1994) 223.
26. J. R. REGALBUTO, K. AGASHE, A. NAVADA, M. L. BRICKER and Q. CHEN, *Studies in Surface Science and Catalysis* **118** (1998) 147.
27. J. ROUQUEROL, D. AVNIR, C. W. FAIRBRIDGE, D. H. EVERETT and J. H. HAYNES, *Pure & Appl. Chem.* **66** (1994) 1739.
28. W. STUMM, in "Chemistry of the Solid-Water Interface" (John Wiley & Sons, New York, 1992) p. 52.
29. V. T. ZASPALIS, PhD thesis, University of Twente, The Netherland, 1990, p. 1.
30. C. J. BRINKER, R. SEHGAL, S. L. HIETALA, R. DESHPANDE, D. M. SMITH, D. LOY and C. S. ASHLEY, *J. Membr. Sci.* **94** (1994) 85.

*Received 27 January 1997*
*and accepted 14 January 1999*